9th ECCOMAS Thematic Conference on the Mechanical Response of Composites
COMPOSITES 2023
G. Catalanotti, H. Petterman and G. Pittaresi (Eds)

EVALUATION OF BEND-TWIST COUPLING IN SHAPE MEMORY ALLOY INTEGRATED FIBER RUBBER COMPOSITES

Achyuth R. Annadata[1*], Anett Endesfelder[2,3], Markus Koenigsdorff[4], Johannes Mersch[1], Thomas Gereke[1], Martina Zimmermann[2,3], Chokri Cherif[1]

[1] Institute of Textile Machinery and High Performance Material Technology, Faculty of Mechanical Science and Engineering, TU Dresden, Germany
[2] Institute of Material Science, Faculty of Mechanical Science Engineering, TU Dresden, Germany
[3] Fraunhofer Institute of Material and Beam Technology (IWS), Dresden, Germany
[4] Institute of Solid State Electronics, Faculty of Electrical and Computer Engineering, TU Dresden, Germany
* achyuth_ram.annadata@tu-dresden.de

Keywords: Bend-Twist coupling, Interactive fiber rubber composites, Smart materials

Summary: *Advancements in textile technologies such as the integration of wire shaped Shape Memory Alloys (SMAs) on to the fabric with the help of Tailored-Fiber-Placement (TFP) method, and weft insertion of SMAs during manufacturing of textiles using knitting machines are helping to create composites capable of bending deformations without any external loads. These advancements laid the foundations for versatile applications especially in soft robotics. One such application is Interactive Fiber Rubber Composites (IFRC). The aim of this project is to evaluate the bend-twist coupling in the IFRC. The SMA reinforced composite is made of polydimethylsiloxane (PDMS) and has two layers of glass fibers stacked upon one another and joined with the help of TFP machine. This work focuses on the simulation of this approach in ANSYS with the Woodworth & Kaliske material model for SMA. The important feature of this model is that the shape memory effect can be achieved for different profiles of SMA, thus eliminating the necessity for a pre-stretch in contrast to the built-in model. The experimental values are evaluated from Multi-DIC technique, which is capable of determining deformations with respect to all directions. A comparative study with simulation and experimental results of the deformation and twisting angles is carried out. The derived conclusions will be helpful in obtaining and evaluating 3D spatial movements in IFRC structures with multiple joints in the future projects.*

1 INTRODUCTION

Actuator integrated composites have created an ecosystem of possibilities to create new concepts capable of revolutionising the idea of soft robotics. There are many actuator materials such as Shape Memory Alloys (SMA), Shape Memory Polymers (SMP), dielectric

elastomers, Magneto-Active Polymers, ionic Electro-Active Polymers (iEAP) etc., with the capabilities of achieving varied actuation mechanisms. Many contributions in terms of efficiency in soft robotics are based predominantly on elastomeric polymers [1]. Smart actuator materials such as SMAs and Electro Active Polymers (EAPs) are capable of converting electrical energy into mechanical work and are suitable to be integrated into soft robotic structures [2]. EAPs have a very high activation strains and high switching frequencies with highly elastic material behaviour, but require high voltages and they also exhibit low mechanical forces. In contrast, SMAs have high energy densities resulting in higher actuation forces [3].

Interactive fiber rubber composites (IFRC) are a class of smart composite structures embedded with actuators and sensors. Recent advancements on integrating the SMAs into the composite, contributed in many soft actuator concepts such as crawler robot [4], jumper robots, flower robots [5], locomotion robots, bio-mimetic robotic hand [6], fish robots, soft robotic hand grippers [7, 8] etc. Advancements in textile technologies created possibilities to embed the actuators like SMAs and EAPs onto the reinforcements before infiltrating with the matrix. The integration of SMA into a structure helps to achieve large deformations. These deformations can be obtained by fixing a pre-strained wire on both ends and by heating the wire while embedded in the composite. Ashir et al. [9, 10, 11] used Tailored Fibre Placement (TFP) method and Open Reed Weaving (ORW) techniques to introduce the SMA wire on and into the textiles achieve deformations with respect to fibre-reinforced composite structures. Lohse et al. [13] used flat knitting technology to insert the SMA wire in the textiles during the knitting process, which allowed it to be inserted without any additional surface coating and the fibres act as the constraints on the SMA. By altering the densities of the fibres, [9] and [13] also worked on developing hinges in the textile area to create gradient stiffness properties at various positions in the composite. However, their work is limited to two-dimensional deformations and till date very few three-dimensional deformable actuators [14, 15, 16] were developed but none with respect to the fibre orientations.

The objective of this work is to evaluate the bend-twist coupling using a defined fibre orientation. The next sections in the article contribute to the methods, process and the functionality of the IFRC structures.

2 Materials and Methods

A pre-strained Nitinol wire of 0.3 mm provided by SAES Getters (20045 Lainate (Milan), Italy) is used in this work along with two component liquid polydimethylsiloxane (PDMS - Sylgard 184^{TM}). The SMA wire is pre-strianed to 4% by the manufacturer and produces an extrinsic two-way shape memory effect in correspondence to the fixing of the two ends of the SMA wire during activation and deactivation. Twill-woven Glass fiber (GF) with 272 tex and a uni-directional (UD) fabric with GF 1750 tex are used as the reinforcement components.

2.1 Experiment

The SMA wire is braided with polyamide yarns in order to avoid a direct contact to the matrix [17]. The manufactured composite has 2 layers of reinforcements. In the bottom

layer, a twill woven glass fabric is used, and in the top layer, a combination of twill woven glass fabric and the UD textile is arranged in such a way, that both the textiles share an equal half as depicted in the Figure 1.

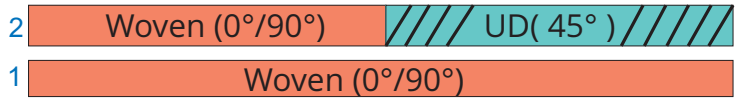

Figure 1: Layout for the reinforcements: layer 1 with complete 0°/90° fibre orientation and layer 2 with partial 0°/90° fibre orientation and partial 45° UD fibres.

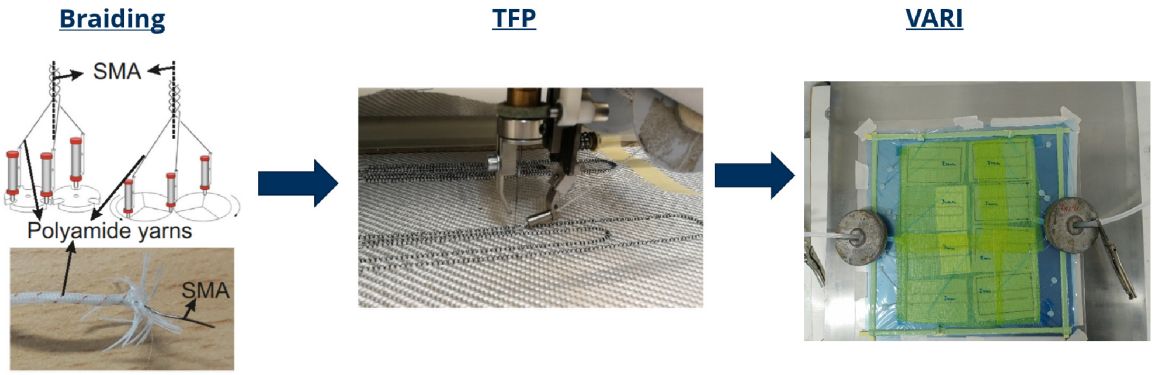

Figure 2: IFRC manufacturing process - Braiding - TFP (Tailored Fibre Placement) - VARI (Vacuum Assisted Resin Infusion)

The whole lay-up is stitched together with the help of Tailored Fibre Placement (TFP) method. A braided SMA is then stitched on top of the lay-up using the TFP method and this semi-finished composite is then infiltrated with liquid silicone using Vacuum Assisted Resin Infusion (VARI) process. The manufacturing process is shown in the Figure 2. The specimens are then cut into the desired dimensions, with a length, width of 120 mm and 80 mm respectively. The thickness of the composite is 2 mm.

The SMA integrated composite is activated at a test bench surrounded with a Multi-Camera-System to capture and analyse the bend-twist coupling with the Digital Image Correlation (DIC). The SMA is activated with the help of Joule heating, by supplying a voltage of 14V with 2A current. The deformations are evaluated using Aramis 5M from GOM, Braunschweig, Germany, with four camera pairs [18]. The images are evaluated using reference points on the sample surface which are projected on to a defined coordinate system and are mapped to track the deformations of the points.

2.2 Modelling

A meso-scale simulation is set-up using Ansys Workbench to predict the deformation behaviour of the SMA integrated fibre rubber composites. The material properties of the SMA wire, PDMS, and the glass fibres are shown in Tables 1,2, 3 and the characterisation methods are briefly explained in [13]. A user-defined model (Woodworth & Kaliske SMA model [19]) is used to solve for the Nitinol SMA wire. The Woodworth & Kaliske model

allows modelling of SMA wires with a pre-defined strain, which allows the user to model different SMA profiles in contrast to modelling only straight SMA wires. Yeoh [12] 3rd order hyper-elastic model is used to model the matrix and the anisotropic properties for the glass fibres are used.

The wire is modelled as a U-profile and is positioned close to the matrix surface to replicate the sample structure. The two ends are fixed and a temperature boundary condition is applied to activate the SMA wire. In place of the braided PA yarns, a hollow polyethylene cylindrical structures is considered, in order to avoid a direct contact between the SMA wire and the matrix. Friction-less contact is considered between the SMA wire and the polyethylene tube, and a bonded contact is given between polyethylene tube and the matrix.

Table 1: Material parameters for Silicone [13].

Model Parameter	**Units**	**Value**
C_{10}	Pa	770623.97
C_{20}	Pa	−386308.55
C_{30}	Pa	196852.40
d_1	Pa^{-1}	0
d_2	Pa^{-1}	0
d_3	Pa^{-1}	0

Table 2: Material parameters for Glass Fibre Yarn [13].

Model Parameter	**Units**	**Value**
elastic modulus in x	GPa	5
elastic modulus in y	GPa	0.04
elastic modulus in z	GPa	0.04
Poisson's ratio (xy)		0.22
Poisson's ratio (yz)		0.22
Poisson's ratio (xz)		0.22
shear modulus (xy)	GPa	0.04
shear modulus (yz)	GPa	0.02
shear modulus (xz)	GPa	0.04

3 Results

3.1 Experiment

Five activation and cooling cycles were coordinated with a heating ramp of 5 seconds and a cooling ramp of 15 seconds for each cycle. Only one surface point at the corner

Table 3: Material parameters for Nitinol wire used for the Woodworth & Kaliske model [19].

Model Parameter	**Units**	**Value at room temperature**
shear modulus of austenite	MPa	9615.4
bulk modulus	MPa	20833
hardening parameter	MPa	610
reference temperature	°C	70
elastic limit	MPa	52
temperature scaling parameter	MPa/°C	7
maximum transformation strain	%	0.0355
shear modulus of martensite	MPa	7692.3
initial martnesite volume fraction	-	0.9
direction of pre-stretch (x,y,z)	-	$(0, 0, 1)$

of the specimen (see Figure: 3b) subjected to the bend-twist coupling is considered and evaluated accordingly. The activation images of the IFRC structure can be seen in Figure 3. The algorithm from the Aramis 5M was able to track the deformations in all three coordinate directions (X,Y and Z). The graph depicting the deformations of the selected point is shown in the Figure 4a and the angle of deformation is shown in the Figure 4b.

3.2 Modelling

Only one heating cycle was simulated because of the resulting high computation time. The directional deformations are plotted in the Figure 5a and the angle of deformation is shown in the Figure 5b. The phase change from martensite to austenite takes place and the volume fraction at the end of the simulation time can be seen in the Figure 6.

4 Discussion

The modelling and the experimental results are compared based on their directional deformations and the deformation angles of the reference point considered. In the experiment, the first activation cycle showed a maximum deformation in the Z-direction, with a deformation value of close to 40 mm and the angle of deformation of 29°. At the end of each cycle, the reference point had an offset in the coordinate system, meaning the composite failed to revertback to the starting point. The rate of deformation increased for the following cycles, but upon careful observations, the amplitude/stroke of each cycle remained the same. The offset is observed because of less cooling time, which is 15 seconds

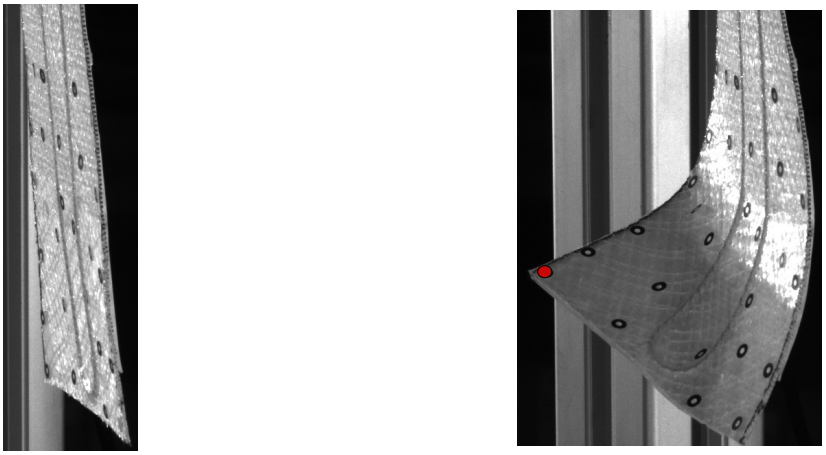

(a) (b)

Figure 3: (a) IFRC before activation, (b) IFRC after activation depicting the reference measuring point (highlighted in red).

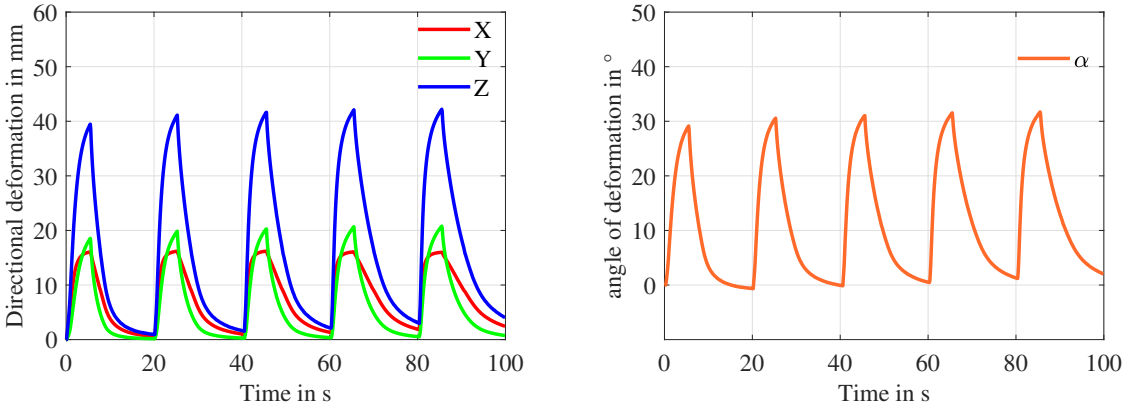

(a) (b)

Figure 4: (a) Directional deformation of the reference point in X,Y and Z directions, (b) angle of deformation (α) of the reference point in degrees.

for each cycle. The X and Y deformations had maximum deformation values of 16 mm and 18 mm respectively in the first cycle. Here, the influence of fibre angle can be clearly seen, by which the deformation in X shows less value compared to the deformation in Y.

In the simulation, the directional deformation in Z resulted in a higher value of 57.8 mm compared to the experiment and the angle of deformation was about 42°. The main plausible reason for the significant difference between the experimental and simulation results is that, the UD fibres in the simulation are bonded in place to the matrix and are not connected with each other. This led to the loss of influence on the deformation, through which the tangential forces which are supposed to be acting on the fibres due to the virtue of the fibre to fibre contact and the SMA wire, produced normal forces resulting in higher deformation values. This can be verified from the graph 5a, in which the X and

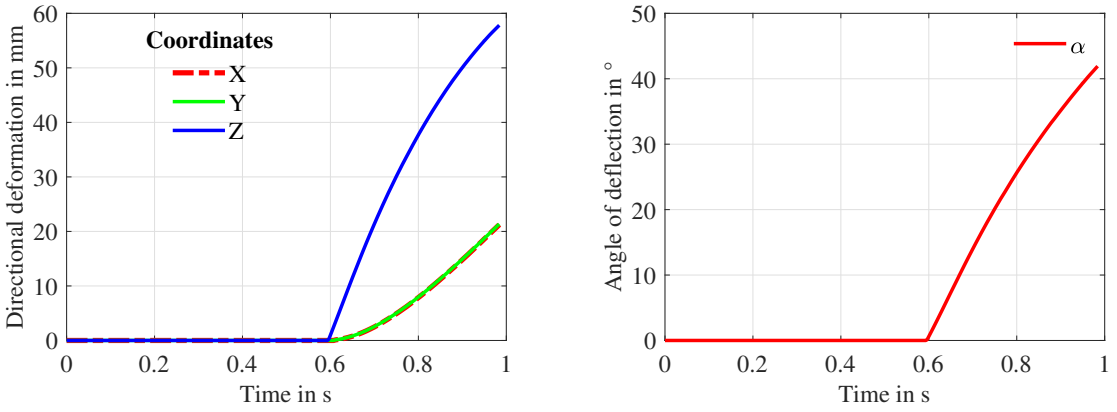

(a) (b)

Figure 5: (a) Directional deformation of the reference point in X,Y and Z directions (simulation), (b) angle of deflection (α) of the reference point in degrees (simulation).

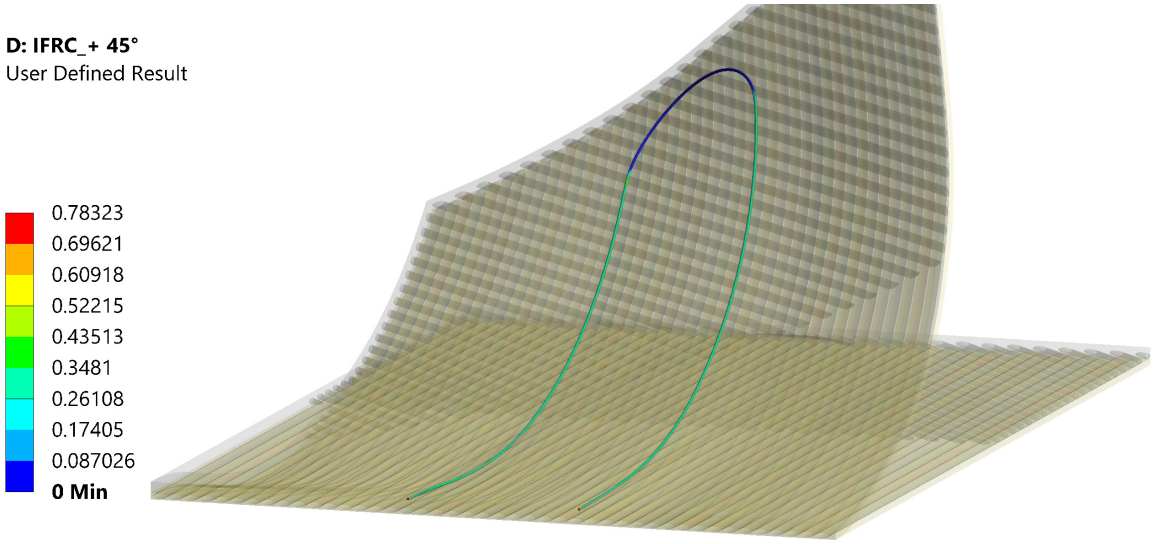

Figure 6: Volume fraction of the SMA wire at the end of heating - martensite (red colour) to austenite (blue colour)

Y deformations share the same space. An attempt was made to assign contacts between each UD fibre and this resulted in higher instability to the finite element problem, creating contact adversities and convergence issues.

5 Conclusion

A shape memory alloy integrated composite capable of bend-twist coupling is fabricated using textile technologies such as braiding and tailored fibre placement method and is then infiltrated with silicone using vacuum assisted resin infusion process. An unconventional fibre lay-up is used to achieve the deformation coupling by stitching the 45° uni-directional

fibres on top of an 0°/90° woven fibre layer. The SMA wire is heated via joule heating and a five cycle activation test was conducted on a DIC test-bench with four camera pairs, which are calibrated to track the marker points placed on the composite in the three-dimensional space. The directional deformations are evaluated at a corner point which is expected to show the maximum deformation due to the orientation of 45° UD fibres. A meso-scale model simulation based on the Woodworth & Kaliske SMA model for SMA wire is carried out to analyse and predict the deformations. A significant difference was observed in the experimental and simulated deformations with the simulation predicting much higher values than anticipated. This is due to the fibres having no direct contact to each other resulting in a very less influence in the tangential direction in the line of force exerted by the SMA. A contact condition with each other between the 45° fibres led to instability to the finite element problem. Further simulation techniques such as coupling of macro-meso models are being pursued to overcome this difficulty. Furthermore, in the experiments only five cycles were pursued. In the future work, the behavioural patterns of the composite will be analysed based on more cyclic testing and affect of overheating on the composite will be reviewed.

Acknowledgement

The DFG research project 380321452/GRK 2430 is supported by the Deutsche Forschungsgemeinschaft (DFG, German Research Foundation). The financial support is gratefully acknowledged. Furthermore, the authors would like to thank Carl Zeiss GOM Metrology GmbH for the loan of the DIC camera system.

REFERENCES

[1] R.F. Shepherd, F. Ilievski, W. Choi, S.A. Morin, A. A. Stokes, A.D. Mazzeo, X. Chen, M. Wang, G.M. Whitesides, Multigait Soft Robot. Proceedings of the National Academy of Sciences of the United States of America. 108. 20400-3. 2011.

[2] A. Verl, A.A. Schäffer, O. Brock, A. Raatz, *Soft robotics: Transferring theory to application.* **01** 2015.

[3] S. Kumar, S. Peruvazhuthi, S. Gopalakrishnan, A half a decade timeline of shape memory alloys in modeling and applications. *ISSS Journal of Micro and Smart Systems*, **9**, 2020.

[4] C.Y. Liu and W.H. Liao, A snake robot using shape memory alloys, In 2004 *IEEE International Conference on Robotics and Biomimetics*, 601-605, 2004.

[5] L.H. Hao, S.H. Park, J.O. Park, Shape memory alloy based flower robot, *39th International Symposium on Robotics*, 2008.

[6] T. Maeno, T. Hino, Miniature five-fingered robot hand driven by shape memory alloy actuators, 174-179, 2006

[7] H. Kim, M.W. Han, S.H. Song, S.H. Ahn, Soft morphing hand driven by sma tendon wire, *Composites Part B: Engineering*, **105**, 2016.

[8] J.H. Lee, Y. Chung, H. Rodrigue, Long shape memory alloy tendon-based soft robotic actuators and implementation as a soft gripper, *Scientific Reports*, **9**, 2019.

[9] M. Ashir, A. Nocke, and C. Cherif. Adaptive fiber-reinforced plastics based on open reed weaving and tailored fiber placement technology. *Textile Research Journal*, 90:004051751988457, 2019.

[10] M. Ashir, A. Nocke, and C. Cherif. Maximum deformation of shape memory alloy based adaptive fiber-reinforced plastics. *Composites Science and Technology*, 184:107860, 2019.

[11] M. Ashir, D.M.P. Vo, A. Nocke, and C. Cherif. Adaptive fiber-reinforced plastics based on open reed weaving functionalization. IOP Conference Series: *Materials Science and Engineering*, 406(1):012063, 2018.

[12] O.H. Yeoh, Some forms of the strain energy function for rubber. *Rubber chem. Technol.* **1993**, 66, 754-771.

[13] F. Lohse, K. Kopelmann, H. Grellmann, M. Ashir, T. Gereke, E. Häntzsche, C. Sennewald, and C. Cherif. Experimental and numerical analysis of the deformation behavior of adaptive fiber-rubber composites with integrated shape memory alloys. *Materials*, **15**, 2022.

[14] H. Rodrigue, W. Wang, B. Bhandari, M.W. Han, and S.H. Ahn. Cross-shaped twisting structure using sma-based smart soft composite. *International Journal of Precision Engineering and Manufacturing-Green Technology*, 1:153–156, 2014.

[15] S.H. Ahn, K.T. Lee, H. Kim, R. Wu, J. Kim, and S.H. Song. Smart soft composite: An integrated 3d soft morphing structure using bend-twist coupling of anisotropic materials. *International Journal of Precision Engineering and Manufacturing*, **13**, 2012.

[16] J.E. Shim, Y.J. Quan, W. Wang, H. Rodrigue, S.H. Song, and S.H. Ahn. A smart soft actuator using a single shape memory alloy for twisting actuation. *Smart Materials and Structures*, 24:125033, 2015.

[17] J. Mersch, C. A. G. Cuaran, A. Vasilev, A. Nocke, C. Cherif and G. Gerlach, "Stretchable and Compliant Textile Strain Sensors," in *IEEE Sensors Journal*, **21**, 25632-25640, 2021.

[18] Carl Zeiss GOM Metrology GmbH, http://www.gom.com/de-de/themen/aramis-multi-sensor-dic-systeme.

[19] L.A. Woodworth, F. Lohse, K. Kopelmann, C. Cherif, M. Kaliske, Development of a constitutive model considering functional fatigue and pre-stretch in shape memory alloy wires, *International Journal of Solids and Structures*, **234–235**, 2022.